

## Transient characteristics of Al x Ga 1x N/GaN heterojunction field-effect transistors

J. Z. Li, J. Y. Lin, H. X. Jiang, and G. J. Sullivan

Citation: *Applied Physics Letters* **77**, 4046 (2000); doi: 10.1063/1.1332412

View online: <http://dx.doi.org/10.1063/1.1332412>

View Table of Contents: <http://scitation.aip.org/content/aip/journal/apl/77/24?ver=pdfcov>

Published by the [AIP Publishing](#)

---

### Articles you may be interested in

[Thermal distributions of surface states causing the current collapse in unpassivated AlGaN GaN heterostructure field-effect transistors](#)

*Appl. Phys. Lett.* **86**, 012106 (2005); 10.1063/1.1844610

[Scanning capacitance spectroscopy of an Al x Ga 1x N/GaN heterostructure field-effect transistor structure: Analysis of probe tip effects](#)

*J. Vac. Sci. Technol. B* **20**, 1671 (2002); 10.1116/1.1491536

[Quantitative analysis of nanoscale electronic properties in an Al x Ga 1x N/GaN heterostructure field-effect transistor structure](#)

*J. Vac. Sci. Technol. B* **19**, 1671 (2001); 10.1116/1.1385914

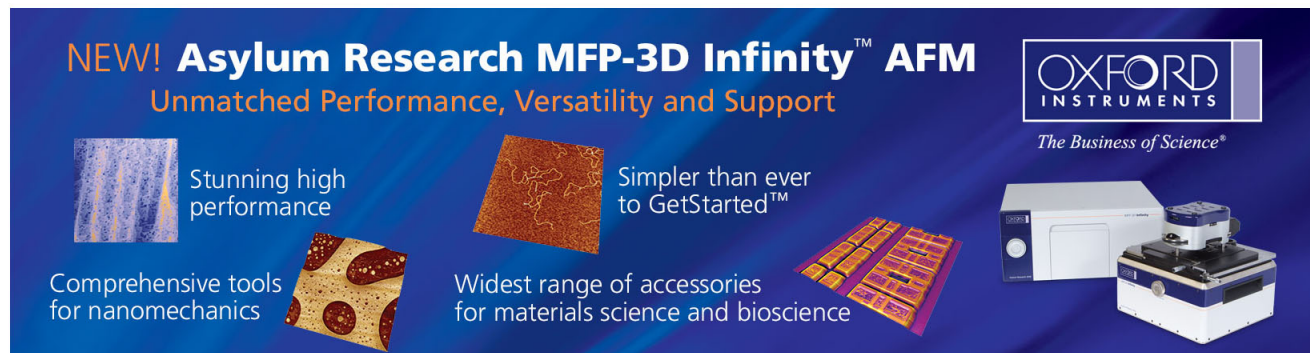
[Two-dimensional electron-gas density in Al X Ga 1X N/GaN heterostructure field-effect transistors](#)

*Appl. Phys. Lett.* **73**, 1856 (1998); 10.1063/1.122305

[Selective wet etching for highly uniform GaAs / Al 0.15 Ga 0.85 As heterostructure field effect transistors](#)

*J. Vac. Sci. Technol. B* **15**, 167 (1997); 10.1116/1.589243

---

The advertisement features a dark blue background with white and orange text. At the top left, it reads 'NEW! Asylum Research MFP-3D Infinity™ AFM' in large white letters, with 'Unmatched Performance, Versatility and Support' in orange below it. On the right, the 'OXFORD INSTRUMENTS' logo is shown in white, with the tagline 'The Business of Science®' underneath. The central part of the ad is divided into four quadrants, each with an image and text: top-left shows a textured surface with the text 'Stunning high performance'; top-right shows a brown, porous-looking surface with 'Simpler than ever to GetStarted™'; bottom-left shows a pattern of red and white circles with 'Comprehensive tools for nanomechanics'; bottom-right shows a grid of small, colorful rectangular samples with 'Widest range of accessories for materials science and bioscience'. On the far right, a photograph of the MFP-3D Infinity AFM instrument is displayed.



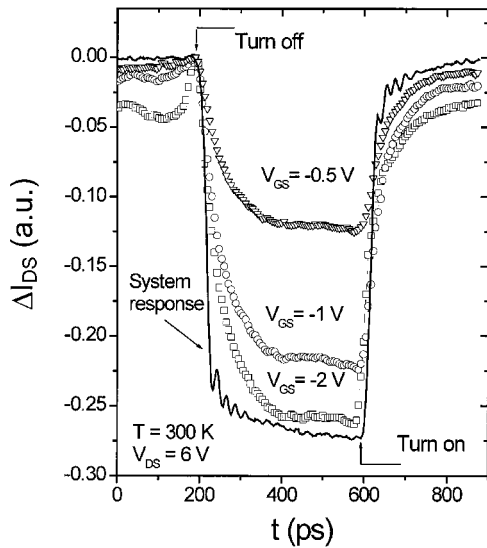


FIG. 2. Drain-source current transient behaviors (or switching-on and -off characteristics) of HFET A measured at  $T=300$  K under a fixed dc drain-source bias ( $V_{DS}=6$  V) for three representative pulsed gate-source voltages  $V_{GS}$ . The system response to the input picosecond square wave pulse is also included and indicated as system response.

analyzer and applied to the gate. The variation of the drain current was displayed and recorded by a 50 GHz sampling digital oscilloscope as a voltage signal.

Devices used in this work were grown by metalorganic chemical vapor deposition, and consisted of a 300 Å Si doped  $n$ -Al<sub>x</sub>Ga<sub>1-x</sub>N layer with  $x\sim 0.25$  and doping concentration of about  $2\times 10^{18}$  cm<sup>-3</sup> on the top of a 2 μm insulating GaN epilayer grown on a sapphire substrate (0001) with a low temperature buffer layer of thickness of about 250 Å. At room temperature, the original wafer exhibited sheet density and mobility of about  $1.7\times 10^{13}$  cm<sup>-2</sup> and 1100 cm<sup>2</sup>/Vs, respectively, as well as a weak effect of PPC. Mesas were formed by reactive ion etching. The gate metallization was prepared by depositing Pt/Au on the top of  $n$ -AlGaN layer. The drain and source ohmic contacts were deposited with bilayers of Ti/Al on the  $n$ -AlGaN top layer and annealed at 950 °C in nitrogen. Ti/Au layers were also used to form air bridges. Two HFETs, labeled A and B shown in Fig. 1(b), were investigated. The gate length ( $L_g$ ) was 0.6 μm for both HFETs and the gate widths ( $W_g$ ) were 37 μm for A and 80 μm for B. Both devices exhibit similar behaviors, while the switching speed of HFET B was slower due to its larger gate area.

Figure 2 shows the drain current transient characteristics in response to pulsed gate-source voltage  $V_{GS}$  measured for HFET A for three representative values of  $V_{GS}=-2.0$ ,  $-1.0$ , and  $-0.5$  V when a 6.0 V dc voltage was applied between source and drain, corresponding to the HFETs normal operating conditions. The response of the system setup to the source pulse is also included in Fig. 2 and labeled as “system response.” Figure 3 plots (a) the switching-off and (b) the switching-on transient kinetics obtained under two representative gate-source voltages ( $V_{GS}=-0.5$  and  $-0.2$  V). The “switching-on” and “switching-off” time constants,  $\tau_{on}$  and  $\tau_{off}$ , were obtained by fitting the transient kinetics to the functions,  $\Delta I = \Delta I_0[1 - \exp(-t/\tau_{on})]$  for the “on” process and  $\Delta I = \Delta I_0[\exp(-t/\tau_{off}) - 1]$  for the “off” process. A de-

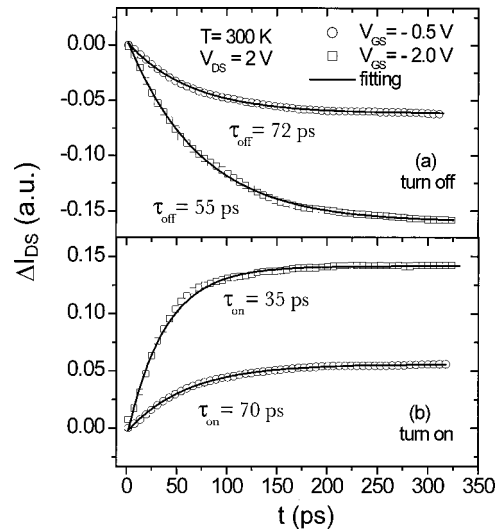


FIG. 3. Drain current transient kinetics of (a) switching-on and (b) switching-off at two representative gate-source voltages. Measured data points have been deconvoluted from the system response. Solid lines are the least squares fitting of data to the functions,  $\Delta I = \Delta I_0[1 - \exp(-t/\tau_{on})]$  for the on process and  $\Delta I = \Delta I_0[\exp(-t/\tau_{off}) - 1]$  for the off process.

convolution method was employed to subtract the system response from the measured signals. As illustrated in Fig. 3, the switching-on and -off time constants are of the order of tens of picoseconds. More interestingly, the deep level trapping effect, which gave rise to a much slower transient ( $\mu$ s) in AlGaAs/GaAs HFETs,<sup>8</sup> was absent in AlGaN/GaN HFETs in the voltage range studied here in spite of the presence of a weak PPC effect in the device structure.

The time constants of the switching-on and -off transients were measured in both the linear ( $V_{DS}<2.5$  V) and saturation regimes ( $V_{DS}>3.5$  V) of the transistors. Figure 4 plots the switching time constants,  $\tau_{on}$  and  $\tau_{off}$  obtained for the HFET A as functions of both  $V_{GS}$  and  $V_{DS}$ . We first notice that, for a fixed  $V_{DS}$ , there exists a gate-source voltage at which  $\tau_{off}$  reaches a minimum value corresponding to

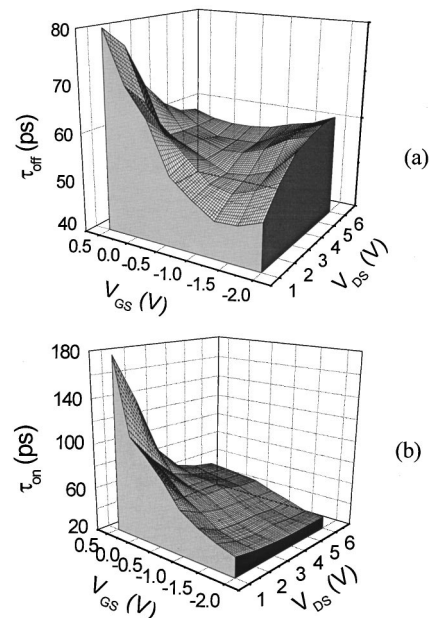


FIG. 4. The switching time constant, (a)  $\tau_{off}$  and (b)  $\tau_{on}$ , as functions of the gate-source bias  $V_{GS}$  and drain-source bias  $V_{DS}$ .

a fastest switching-off speed. This behavior is a mirror image of the gate-source voltage dependence of the mobility in AlGaN/GaN HFET structures,<sup>9</sup> in which a maximum mobility occurs at a negative gate-source voltage. We thus believe that the systematic dependence of the switching-off time constant on the gate-source voltage is primarily determined by the behavior of the effective electron mobility in the channel.

It has been demonstrated that the mobility ( $\mu$ ) in AlGaAs/GaAs or AlGaIn/GaN heterostructures depends strongly on the effective sheet density ( $n_s$ ), which increases with the gate-source voltage.<sup>10,11</sup> The mobility  $\mu$  increases with an increase of  $n_s$  due to an enhanced carrier screening at  $n_s < n_c$  and reaches a maximum at  $n_s \sim n_c$ , where  $n_c$  ( $\sim 1 \times 10^{15} \text{ cm}^{-2}$  in Al<sub>0.25</sub>Ga<sub>0.85</sub>N/GaN HFETs) is defined as the maximum sheet density at which the electrons are still confined in the two-dimensional (2D) channel.<sup>12</sup> As the gate-source voltage further increases (or becomes less negative), the effective mobility  $\mu$  decreases with further increasing  $n_s$  due to the electrons spillover from the 2D channel and an enhanced parallel conductance in the lower-mobility AlGaIn layer. In AlGaIn/GaN HFETs, both the large conduction band offset and the piezoelectric field<sup>12-14</sup> have resulted in a fairly high sheet density in the channel region. In the device structures used here,  $n_s \sim 1.7 \times 10^{13} \text{ cm}^{-2}$  ( $> n_c$ ) at  $V_{GS} = 0$ . Thus a maximum mobility and fastest switching speed occur at a negative gate-source voltage that varies with the drain-source voltage. This is illustrated in Fig. 4(a).

Figure 4(b) shows that the switching-on time constant  $\tau_{on}$  decreases monotonically with a decrease of the gate-source voltage. This behavior seems to suggest that  $\tau_{on}$  is dominated by the gate-source capacitance which increases with increasing gate-source voltage  $V_{GS}$ . At  $V_{GS} > 0$ , the gate-source capacitance results primarily from the induced electrons in the region of AlGaIn epilayer near the heterointerface.<sup>15</sup> On the other hand, the dependence of the switching speed on the source-drain voltage,  $\tau$  vs  $V_{DS}$ , is expected to be dominated by the drain-source voltage dependence of the electron drift velocity, which is an increasing function under low fields. Thus both  $\tau_{on}$  and  $\tau_{off}$  are expected to decrease with an increase of  $V_{DS}$ . This was indeed the behavior observed for the switching-on time constant  $\tau_{on}$  as shown in Fig. 4(b). However, the increase of the switching-off time constant with  $V_{DS}$  in the negative gate-source voltage region shown in Fig. 4(a) requires further understanding.

Our studies indicate that the switching speed of AlGaIn/GaN HFETs is directly related to the effective mobility as well as the gate-source capacitance and varies under different bias conditions. It has been suggested that the use of higher Al contents and higher doping concentrations (and thus higher  $n_s$ ) in the AlGaIn barrier layers could improve the HFET power output.<sup>16</sup> Our results indicate that there may be a trade off between the output power and switching speed. Additionally, the degradation of the Al<sub>x</sub>Ga<sub>1-x</sub>N epilayer

crystalline quality at higher Al contents and high doping levels can result in a higher density of parasitic charges, which could lead to a larger gate-source capacitance and thus a longer switching time. Therefore, the channel sheet density should be properly optimized. The recently reported doped-channel AlGaIn/GaN HFET designs have demonstrated a lower parasitic electron concentration as well as an enhanced sheet density and transconductance.<sup>11,17</sup> These features are promising for improving both the device switching speed and the power output.

In summary, the drain-source current transients in response to picosecond pulsed gate-source voltages in Al<sub>x</sub>Ga<sub>1-x</sub>N/GaN HFETs have been measured. Though experimental results were discussed qualitatively in terms of the variations of the electron sheet density, effective mobility, and gate-source capacitance during the switching-on and -off processes, they provided new insights for theoretical modeling which could lead to a more quantitative understanding. More measurements at higher fields as well as to include different structural designs are still needed.

The research is supported by grants from BMDO (monitored by USASMD) and DOE (Grant No. 96ER45604/A000). The authors are grateful to Professor R. Hui for his help with the high speed measurements.

- <sup>1</sup>A. T. Ping, Q. Chen, J. W. Yang, M. A. Khan, and I. Adesida, *IEEE Electron Device Lett.* **19**, 54 (1998).
- <sup>2</sup>B. Gelmont, K. S. Kim, and M. Shur, *J. Appl. Phys.* **74**, 1818 (1993).
- <sup>3</sup>M. A. Khan, Q. Chen, M. S. Shur, B. T. Dermott, J. A. Higgins, J. Burm, W. J. Schaff, and L. F. Eastman, *IEEE Electron Device Lett.* **17**, 584 (1996).
- <sup>4</sup>Y. F. Wu, B. P. Keller, S. Keller, N. X. Nguyen, M. Le, C. Ngyen, T. J. Jenkins, L. T. Kehias, S. P. DenBaars, and U. K. Mishra, *IEEE Electron Device Lett.* **18**, 438 (1997).
- <sup>5</sup>J. Z. Li, J. Y. Lin, H. X. Jiang, M. A. Khan, and Q. Chen, *J. Appl. Phys.* **82**, 1227 (1997).
- <sup>6</sup>J. Z. Li, J. Li, J. Y. Lin, and H. X. Jiang, *Mater. Res. Soc. Symp. Proc.* **595**, W11.12 (1999).
- <sup>7</sup>P. M. Mooney, *J. Appl. Phys.* **67**, R1 (1990).
- <sup>8</sup>M. I. Nathan, P. M. Mooney, P. M. Solomon, and S. L. Wright, *Appl. Phys. Lett.* **47**, 628 (1985).
- <sup>9</sup>X. Z. Dang, P. M. Asbeck, E. T. Yu, G. J. Sullivan, M. Y. Chen, B. T. McDermott, K. S. Boutros, and J. M. Redwing, *Appl. Phys. Lett.* **74**, 3890 (1999).
- <sup>10</sup>S. M. Liu, M. B. Das, W. Kopp, and H. Morkoc, *IEEE Electron Device Lett.* **EDL-6**, 594 (1985).
- <sup>11</sup>R. Gaska, M. S. Shur, A. D. Bykhovski, A. O. Orlov, and G. L. Snider, *Appl. Phys. Lett.* **74**, 287 (1999).
- <sup>12</sup>R. Gaska, J. Yang, A. Osinsky, A. D. Bykhovski, and M. S. Shur, *Appl. Phys. Lett.* **71**, 3673 (1997).
- <sup>13</sup>E. T. Yu, G. J. Sullivan, P. M. Asbeck, C. D. Wang, D. Qiao, and S. S. Lau, *Appl. Phys. Lett.* **71**, 2794 (1997).
- <sup>14</sup>L. Hsu, W. Walukiewicz, R. Oberhuber, G. Zandler, and P. Vogl, *Appl. Phys. Lett.* **73**, 339 (1998).
- <sup>15</sup>N. Mohammad, Z. F. Fan, A. Salvador, O. Aktas, A. E. Botchkarev, W. Kim, and H. Morkoc, *Appl. Phys. Lett.* **69**, 1420 (1996).
- <sup>16</sup>Y. F. Wu, B. P. Keller, P. Fini, S. Keller, T. J. Jenkins, L. T. Kehias, S. P. DenBaars, and U. K. Mishra, *IEEE Electron Device Lett.* **19**, 50 (1998).
- <sup>17</sup>S. Imanaga and H. Kawai, *J. Appl. Phys.* **82**, 5843 (1997).